



Study of the stir speed and time in AA6030 matrix reinforced with Al_2O_3 nanoparticles

M. E. Mendoza-Oliveros^{a*} • A. K. Jimenez-Miguez^a • Y. Bautista-Vargas^a •
B. S. Archanjo^b • C. A. Senna^b • L. Mujica-Roncery^a • N. Rojas-Arias^{a,c**}

^aUniversidad Pedagógica y Tecnológica de Colombia.
Avenida Central del Norte 39-115 - P.O. Box 150001, Boyacá, Colombia

^bNational Institute of Metrology Quality and Technology (INMETRO),
Materials Metrology Division (DIMAT), Brazil

^cPostgraduate Program in Materials Science and Engineering,
Federal University of São Carlos 1356-905, São Carlos, Brazil

Received 06 02 2021; accepted 09 30 2021

Available 02 28 2022

Abstract: The effect of speed and time of stirring for AA6063 matrix manufactured by Electric Induction Furnace and reinforced 0.75wt.% and 1.5wt.% of Al_2O_3 nanoparticles is studied. The specimens produced were subjected to tensile, microhardness, and tribology tests. It is observed that an increase in the speed and agitation time for AA6063 samples reinforced with 0.75%, favors an increase in the grain size, while an opposite effect is observed with the parts produced with 1.5%, where a grain refining effect is favored, affecting the mechanical properties of the reinforced alloy. The data obtained in this work show that the stirring speed and time will depend on the content of reinforcing particles used in the alloy

Keywords: AA6063 matrix, Al_2O_3 nanoparticles, speed and time of stirring, mechanical properties

*Corresponding author.

E-mail address: martin.mendoza@uptc.edu.co, nicolas.rojas@estudante.ufscar.br (M. E. Mendoza-Oliveros, N. Rojas-Arias).

Peer Review under the responsibility of Universidad Nacional Autónoma de México.

1. Introduction

Metal matrix nanocomposites provide new opportunities for the design of new structures, improving their tribological performance, as well as their mechanical and physical properties (Cabeza et al., 2017; Casati et al., 2015; Tjong, 2007). The aluminum matrix reinforced with alumina nanoparticles are of great interest in applications such as structural systems, car brake discs, combustion engines, so on. However, the processing of these composite materials presents complexities depending on the production method (Koli et al., 2014). The application of nanoparticles as reinforcement material allows a higher surface / volume ratio (up to 1000 times more) compared to the application of microparticles, allowing to obtain a greater reinforcement and optimization of the mechanical properties (Madhukar et al., 2016; Madhukar et al., 2019).

In general, for the synthesis of these nanocomposites, powder processing methods are used followed by compaction and sintering processes, high mechanical deformation, or production of nanocomposites in the form of coatings via electrodeposition or PVD. Nevertheless, the application of casting and stirring processes have had a great impact because these have implied a greater production of this type of material, as well as adaptation to different shapes and sizes of parts depending on the casting molds (Koli et al., 2014). In addition, stir casting is an inexpensive process that allows the use of different types of alloys, highlighted to manufacture bulk quantities of reinforced parts. (Bhowmik et al., 2021; Jiang & Wang, 2015).

It is expected that in casting processes a suitable bond between the matrix and the nanoparticles is obtained (Akbari et al., 2013; Mazahery & Ostadshabani, 2011). However, the properties of the reinforced part can be subject to process factors such as speed, and stirring time of the molten compound (Liu et al., 2020). Mechanical stirring mixes the ceramic particles into the molten metal. When the agitation is stopped the particles tend to sink, float, or agglomerate in a non-homogeneous way (Akbari et al., 2013). A homogeneous arrangement of the nanoparticles plays an important role on the mechanical behavior of reinforced parts, for which it is necessary to determine the optimal conditions during the manufacturing processes of alloys reinforced by casting processes. Due to this, the aim of this work is focused on studying the effect of the time and speed of stirring of the metal bath on the tribological, physical, and tensile properties of AA6063 parts reinforced with two percentages of alumina nanoparticles. The work contributes that the agitation speed and time for the smallest fraction used is decisive for the final mechanical properties. In addition, a great contribution is made by presenting wear results which can be taken into account by the industrial sector, as well as results of comparison with other investigations.

2. Experimental

The AA6063 specimens reinforced with Al₂O₃ nanoparticles (Al₂O₃-np) were manufactured in an Electric Induction Furnace with a built-in mechanical stirring system. The Al₂O₃-np (10 – 50 nm particle size) were characterized in a TEM FEI-Tecnai Spirit at 120kV in bright field, dark field, and electron diffraction modes, as well as by XRD using a Panalytical diffractometer with Co K α radiation ($\lambda = 1.75 \text{ \AA}$). The Al₂O₃-np were added into the AA6063 melted at 700 °C in quantities of 0.75 wt.% and 1.5 wt.%, stirred at 350 RPM and 600 RPM during 5 min and 10 min, respectively. The molten material was poured into 1" x 1/2" rectangular metal molds with a height of 8". Although the addition of Al₂O₃-np is shown as an excellent candidate to optimize the mechanical properties of aluminum parts produced by stirring, (Kandpal et al., 2017; Mohanavel et al., 2018), it was decided to add a low content of nanoparticles in order to avoid the formation of agglomerations, while observing the effect of reinforcing the matrix with a low content of nanoparticles.

The specimens produced were prepared metallographically, and analyzed in a SEM Leo-430 at 20Kv. Mechanical properties were evaluated using microhardness tests at 500gf for 10s, and tensile tests on a universal Microtest EM2/500/FR machine according to ASTM B557-02A. Additionally, tribology tests were evaluated using the pin-on-disk technique according to ASTM G99-04, applying a force of 10N at 120RPM, with a distance of 500m and 2mm footprint radius. A total of three replicates were made for each trial.

3. Results and discussion

Figure 1(a) shows the XRD pattern obtained. The data show that the nanoparticles correspond to γ - Al₂O₃, presenting a space group $Fd\bar{3}m$ (227) with lattice parameters 7.932 Å, and an angle of $\alpha = \beta = \gamma = 90^\circ$ (Cod. 1101168); corundum is presented lattice parameters $a = 4.805 \text{ \AA}$, $b = 4.805 \text{ \AA}$, and $c = 13.116 \text{ \AA}$, and angles of $\alpha = \beta = 90^\circ$ and $\gamma = 120^\circ$ (Cod. mp-1143); and θ - Al₂O₃ with a space group $c2/m$, lattice parameters $a = 11.985 \text{ \AA}$, $b = 2.91 \text{ \AA}$, and $c = 5.621 \text{ \AA}$, and angles of $\alpha = \gamma = 90^\circ$ and $\beta = 103.79^\circ$ (Cod. mp-7084). Furthermore, laser particle scattering tests were performed using isopropyl alcohol as the dispersing agent and accompanied by TEM technique. Figure 1(b – d) show a set of bright and dark field images of Al₂O₃-np with its corresponding diffraction pattern. At lower magnification Al₂O₃-np aggregates in the 50 nm – 700 nm range were observed. At higher magnification it was possible to show the rod-shaped morphology presented by the Al₂O₃-np. The diffraction patterns inset presented well-defined rings, indicating a polycrystalline structure with small crystal sizes. The red circles indicate the reflection used to obtain the respective dark field. The indexing of the diffraction patterns

determined that the Al_2O_3 -np correspond to the gamma phase, corroborating the results obtained by XRD. Particle size was measured in the dark field images. Figure 1(d) presents the particle size distribution for the Al_2O_3 -np. The results obtained show a particle size between 5nm–50nm, with an average size of 24 ± 10 nm.

Figure 2 shows the microstructural change and the grain size of the built parts. The grain Size was obtained according to ASTM E-112 for each specimen, which is presented in Figure 3. A growth in grain size is produced by the increasing in the stirring speed for specimens with 0.75wt.% Al_2O_3 -np, while specimens with 1.5wt.% Al_2O_3 -np show an opposite effect, obtaining the minor value of up to $78.54 \mu\text{m}$ for the AA6063 reinforced with 1.5wt.% Al_2O_3 -np at 600RPM during 10min.

The unreinforced AA6063 parts had an average grain size of $52 \mu\text{m}$. The addition of Al_2O_3 -np generates a refining effect in most of the parts produced. The parts produced with 0.75 wt.% Al_2O_3 -np lose their refining effect when stirring time and speed is increased, obtaining an optimal grain size at 350 RPM/5min. In contrast, the parts reinforced with 1.5 wt.% Al_2O_3 -np show an opposite effect, increasing the refining effect by increasing the time and speed of stirring. The variation of the average size of the built parts is shown in Fig. 3. This decreasing can be accompanied by a potential increase in dislocation density at the interface between the nanoparticles and the matrix, due to the mismatch of coefficients of thermal expansion (Abbasipour et al., 2019). It has been shown that the addition of ceramic nanocomposites to metallic matrices can reduce the average size of precipitates and grains of a metallic matrix (Kandpal et al., 2017; Liu et al., 2020); nevertheless, the addition of a higher content of nanoparticles will require a greater time and speed of agitation to ensure their homogenization within the part and thus obtain the refining effect that favors the mechanical properties of the alloy.

Table 1 shows the data from the mechanical tests obtained in this work. The microhardness values reflect a considerable increase higher when adding Al_2O_3 -np. The addition of Al_2O_3 -np generates an increase in the Hardness of all the reinforced samples. The maximum Hardness values were obtained for the parts with addition 0.75wt.% / 350RPM / 5min (33.7 % increase) and 1.5wt. % Al_2O_3 -np at 600RPM / 10min (32.8 % increase) while the lowest Hardness value was obtained in the reinforced parts with 1.5wt.% Al_2O_3 -np at 350RPM / 5min (15.5 % increase). The variation of the hardness is directly related with the obstruction of the movement of dislocations,

allowing to strengthen the Orowan mechanism (Casati et al., 2015) and the grain size (Akbari et al., 2013; Mazahery & Ostadshabani, 2011; Sajjadi et al., 2011). In this case the reduction in hardness in Specimens with 1.5wt.% Al_2O_3 -np is mainly associated with an increase in grain size as reported by Abbasipour et al. (2019).

The tensile stress curves are presented in Figure 4(a). For Specimens containing 1.5wt.% Al_2O_3 -np, slightly higher values of UTS and YS were observed in relation to Specimens AA6063 without Al_2O_3 -np. The stir speed and time do not present a relevant influence on the tensile properties in the Specimens produced with 1.5wt.% Al_2O_3 -np, obtaining average values of UTS = 118.24 ± 11 MPa and YS = 81.15 ± 2 MPa, both closed to AA6063 specimens without Al_2O_3 -np. On the other hand, the Specimens produced with 0.75wt.% Al_2O_3 -np show a decrease in tensile properties by increasing the speed of stirring, reaching a reduction of up to 50.1 % in UTS and 44.3 % in YS in AA6063 specimens reinforced with 0.75 wt.% Al_2O_3 -np, using a speed stirring of 600RPM during 10min.

In Figure 4(b) the fracture mechanism for parts reinforced with 0.75wt.% Al_2O_3 -np built with a speed stirring of 600 RPM during 10 min is observed. It is possible to see the presence of Al_2O_3 -np agglomerates, accompanied by other imperfections in the structure of the material can cause an early cracking of the part, favoring the formation and propagation of microcracks in the sample in the form of a partially brittle fracture (Dareini et al., 2020). The EDS images (Figure 4(c – f)) show that the fracture zone has a high content of Al_2O_3 -np and regions with a high content of oxygen and magnesium, mainly in the form of agglomerates, which favored the formation and propagation of cracks (Zaiemyekeh et al., 2019). the presence of oxide agglomerations favors the formation of areas conducive to the production and propagation of cracks that allow the part to fracture.

The values obtained within the tribology tests show that the addition of Al_2O_3 -np to the AA6063 matrix, the increase in stirring speed, and time have a positive effect on the tribological properties of the material. Insufficient stirring speed and time can cause agglomerations of the particles in AA6063 specimens reinforced with 1.5wt.% Al_2O_3 -np, generating a higher rate of wear. The presence of agglomerations generates adhesion and delamination effects, facilitating a greater degree of wear in this type of parts, produced by liquid metallurgy (Abbasipour et al., 2019).

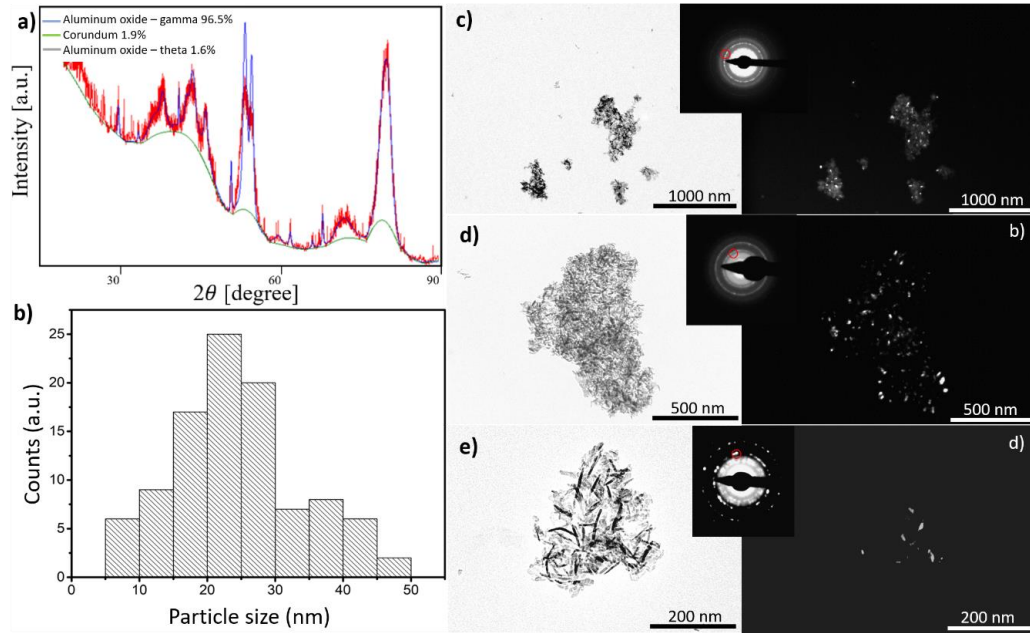


Figure 1. Analysis of the composition and size of alumina particles. In a) XRD pattern, b) particle size distribution and c-e) TEM images of the alumina nanoparticles used in this work.

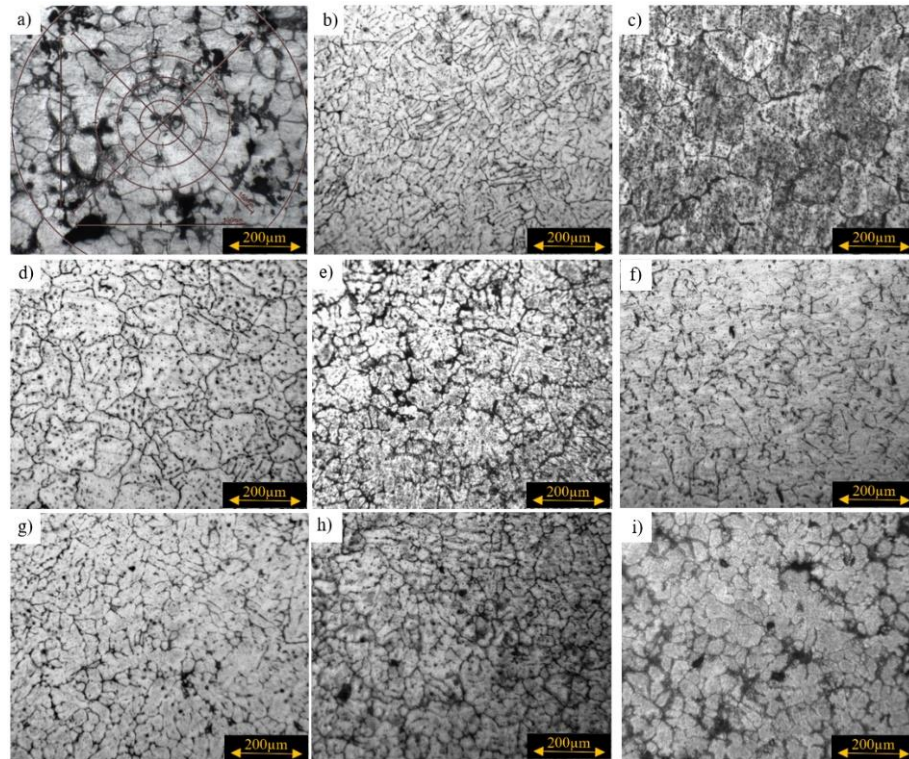


Figure 2. Optical microscope images of AA6063 reinforced with Al₂O₃-np. In a) without reinforcement, b) 0.75 wt.% Al₂O₃-np at 350 RPM/5min, c) 0.75 wt.% Al₂O₃-np at 600 RPM/5min, d) 1.5 wt.% Al₂O₃-np / 350RPM/5min, e) 1.5 wt.% Al₂O₃-np at 600RPM/5min, f) 0.75wt. % Al₂O₃-np at 350RPM/10min, g) 0.75 wt.% Al₂O₃-np at 600RPM/10min, h) 1.5 wt.% Al₂O₃-np at 350RPM/10min and e) 1.5 wt.% Al₂O₃-np at 600RPM/10min.

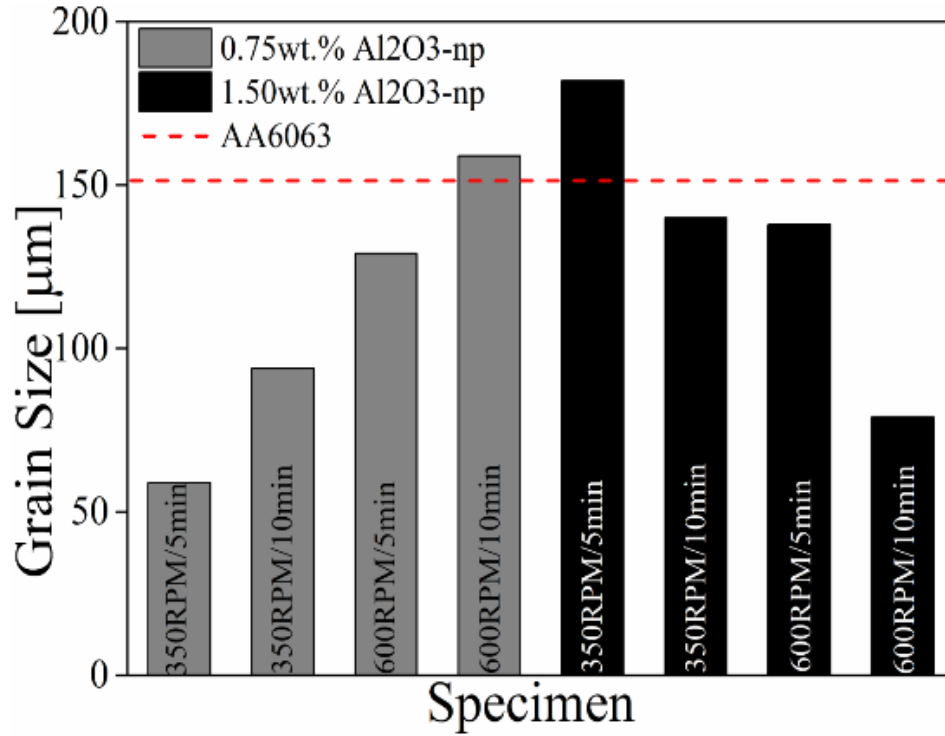


Figure 3. Grain size obtained ASTM E-112 for AA6063 specimens reinforced with Al₂O₃-np and AA6063 unreinforced.

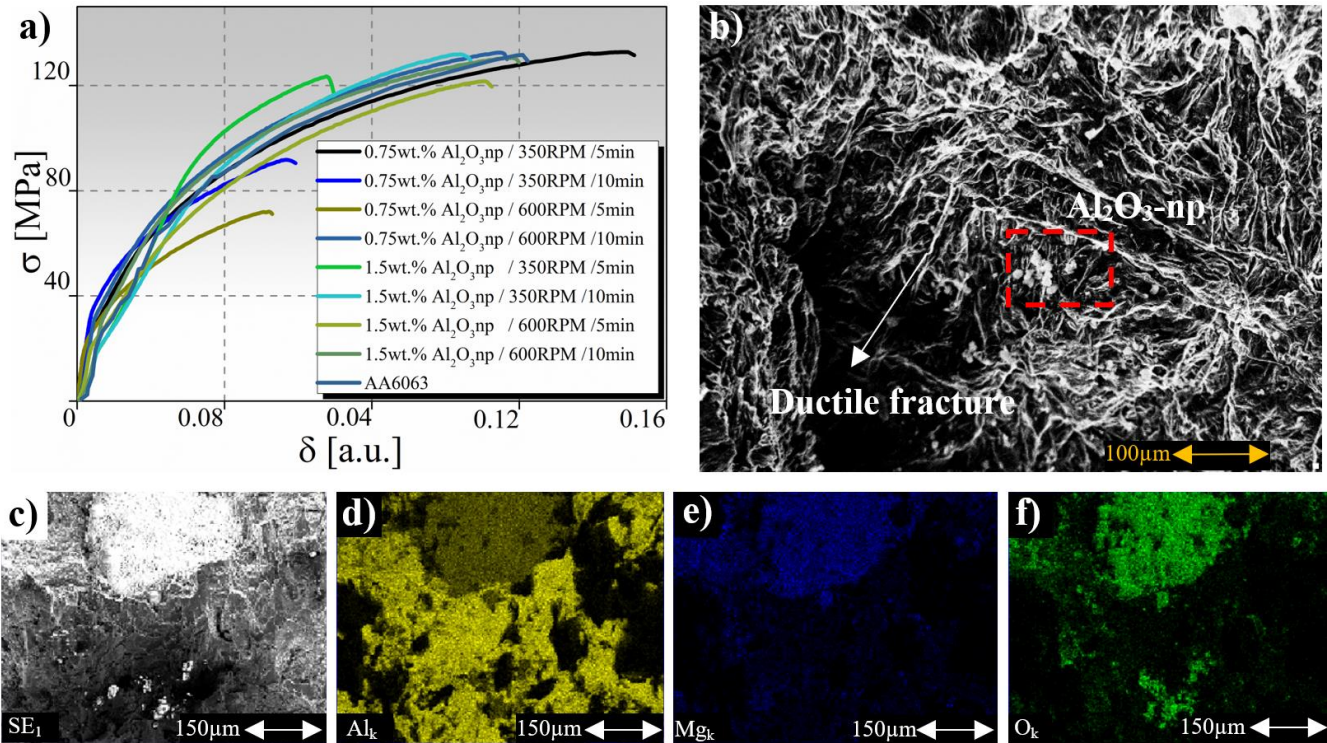


Figure 4. Tensile curves and fractography test developed for AA6063 specimens reinforced with Al₂O₃ nanoparticles. In a) stress vs deformation curves, b) micrograph of brittle fracture of one of the worked specimens and c-f) EDS performed on a fractured area.

Table 1. Values of the mechanical properties.

Al ₂ O ₃ np	[wt.%]	Stir. [RPM]	Time [min]	Hardness [HV]	UTS [MPa]	YS [MPa]	Ductility [%]	F.C.* [a.u.]
0.75	350		5	55.1	117.09 ±16.66	76.67 ±6.4	4.15 ±0.32	0.2772
			10	53.8	97.00 ±12.08	67.56 ±6.9	3.5 ±1.2	0.3239
	600		5	51.4	75.07 ±15.13	50.47 ±8.2	2.28 ±0.13	0.3242
			10	56.4	64.91 ±5.33	44.24 ±3.38	2.43 ±0.2	0.3493
1.5	350		5	47.6	113.15 ±3.65	87.23 ±2.74	3.4 ±0.1	0.3903
			10	53.3	125.98 ±3.22	85.77 ±1.06	3.76 ±0.55	0.3466
	600		5	53.4	114.51 ±3.91	72.23 ±2.19	3.77 ±0.37	0.3336
			10	54.7	119.31 ±7.87	79.38 ±3.04	3.56 ±0.16	0.3218
AA6063				41.2	130.02 ±2.59	79.49 ±2.12	4.55 ±0.42	0.4154

4. Conclusions

The stir casting technique was successfully adopted in the preparation of metallic composites, containing 0.75wt.% and 1.5wt.% of Al₂O₃ powder reinforcement. This technique is influenced by the speed and stirring time of the nanoparticles within the liquid metal. The Specimens produced with a higher rate of speed and stirring time showed a decrease in grain size when adding 1.5wt.%Al₂O₃-np, and an increase in grain size for specimens manufactured with 0.75wt.%Al₂O₃-np. This factor directly affects the hardness of the material, which decreases with an increasing of the grain size.

The values of UTS, YS, and ductility of the AA6063 specimens are affected by adding Al₂O₃-np due to the presence of agglomerations of the nanoparticles, which favored the formation and propagation of cracks that allowed a brittle fracture mechanism. Nevertheless, tribology tests showed a significant improvement in wear resistance, obtaining the best results in specimens produced with 0.75 wt.% Al₂O₃-np. Likewise, an increase in the speed and stirring time allows a reduction of up to 33% of the friction coefficient of the material, compared to the AA6063 Specimens without reinforcement. This allowed an improvement in the wear resistance of the material.

The results obtained in this study allow to demonstrate that the addition of low Al₂O₃-np contents favors a microstructural variation and on the mechanical properties of reinforced aluminum parts using the technique of molten metal stirring processes. The addition of 0.75 wt.% Al₂O₃-np with low revolutions and stirring times allows an optimal refinement of the grain size, favoring the mechanical properties of the piece. The increase in stirring speed and time reduces the refining effect of Al₂O₃-np. In contrast, an increase in the Al₂O₃-np content will require a greater speed and stirring time to homogeneously distribute the Al₂O₃-np in the alloy.

Conflict of interest

The author(s) does/do not have any type of conflict of interest to declare.

Acknowledgments

The support given by the *National Institute of Metrology Quality and Technology (INMETRO -Brazil)*, the *Materials Metrology Division (DIMAT- Brazil)*, and the *Universidad Pedagógica y Tecnológica de Colombia (UPTC - Colombia)*, by providing material and equipment necessary for the research is greatly appreciated.

Financing

The authors did not receive any sponsorship to carry out the research reported in the present manuscript.

References

- Abbasipour, B., Niroumand, B., Monir Vaghefi, S. M., & Abedi, M. (2019). Tribological behavior of A356-CNT nanocomposites fabricated by various casting techniques. *Transactions of Nonferrous Metals Society of China*, 29(10), 1993–2004. [https://doi.org/10.1016/S1003-6326\(19\)65107-1](https://doi.org/10.1016/S1003-6326(19)65107-1)
- Bhowmik, A., Dipankar Dey, & Biswas, A. (2021). *Microstructure, mechanical and wear behaviour of Al7075/SiC aluminium matrix composite fabricated by stir casting. Indian Journal of Engineering and Materials Sciences*, 28(1), 46–54.
- Cabeza, M., Feijoo, I., Merino, P., Pena, G., Pérez, M. C., Cruz, S., & Rey, P. (2017). Effect of high energy ball milling on the morphology, microstructure and properties of nano-sized TiC particle-reinforced 6005A aluminium alloy matrix composite. *Powder Technology*, 321, 31–43. <https://doi.org/10.1016/j.powtec.2017.07.089>
- Casati, R., Fabrizi, A., Tuissi, A., Xia, K., & Vedani, M. (2015). ECAP consolidation of Al matrix composites reinforced with in-situ γ -Al₂O₃ nanoparticles. *Materials Science and Engineering: A*, 648, 113–122. <https://doi.org/10.1016/j.msea.2015.09.025>
- Dareini, M., Jabbari, A. H., & Sedighi, M. (2020). Effect of nano-sized Al₂O₃ reinforcing particles on uniaxial and high cycle fatigue behaviors of hot-forged AZ31B magnesium alloy. *Transactions of Nonferrous Metals Society of China*, 30(5), 1249–1266. [https://doi.org/10.1016/S1003-6326\(20\)65293-1](https://doi.org/10.1016/S1003-6326(20)65293-1)
- Jiang, J., & Wang, Y. (2015). Microstructure and mechanical properties of the semisolid slurries and rheoformed component of nano-sized SiC/7075 aluminum matrix composite prepared by ultrasonic-assisted semisolid stirring. *Materials Science and Engineering: A*, 639, 350–358. <https://doi.org/10.1016/j.msea.2015.04.064>
- Kandpal, B. C., Kumar, J., & Singh, H. (2017). Fabrication and characterisation of Al₂O₃/aluminium alloy 6061 composites fabricated by Stir casting. *Materials Today: Proceedings*, 4(2), 2783–2792. <https://doi.org/10.1016/j.matpr.2017.02.157>
- Akbari, M. K., Mirzaee, O., & Baharvandi, H. R. (2013). Fabrication and study on mechanical properties and fracture behavior of nanometric Al₂O₃ particle-reinforced A356 composites focusing on the parameters of vortex method. *Materials & Design*, 46, 199–205. <https://doi.org/10.1016/j.matdes.2012.10.008>
- Koli, D. K., Agnihotri, G., & Purohit, R. (2014). A Review on Properties, Behaviour and Processing Methods for Al- Nano Al₂O₃ Composites. *Procedia Materials Science*, 6, 567–589. <https://doi.org/10.1016/j.mspro.2014.07.072>
- Liu, X., Zhao, Q., & Jiang, Q. (2020). Effects of cooling rate and TiC nanoparticles on the microstructure and tensile properties of an Al-Cu cast alloy. *Materials Science and Engineering: A*, 790, 139737. <https://doi.org/10.1016/j.msea.2020.139737>
- Madhukar, P., Selvaraj, N., & Rao, C. S. P. (2016). Manufacturing of aluminium nano hybrid composites: a state of review. *In IOP Conference Series: Materials Science and Engineering*, 149 (1), 012114. <https://doi.org/10.1088/1757-899X/149/1/012114>
- Madhukar, Pagidi, Selvaraj, N., Gujjala, R., & Rao, C. S. P. (2019). Production of high performance AA7150-1% SiC nanocomposite by novel fabrication process of ultrasonication assisted stir casting. *Ultrasonics Sonochemistry*, 58, 104665. <https://doi.org/10.1016/j.ultsonch.2019.104665>
- Mazahery, A., & Ostadshabani, M. (2011). Investigation on mechanical properties of nano-Al₂O₃ -reinforced aluminum matrix composites. *Journal of Composite Materials*, 45(24), 2579–2586. <https://doi.org/10.1177/0021998311401111>
- Mohanavel, V., Suresh Kumar, S., Mariyappan, K., Ganeshan, P., & Adithiyaa, T. (2018). Mechanical behavior of Al-matrix nanocomposites produced by stir casting technique. *Materials Today: Proceedings*, 5(13), 26873–26877. <https://doi.org/10.1016/j.matpr.2018.08.170>
- Sajjadi, S. A., Ezatpour, H. R., & Beygi, H. (2011). Microstructure and mechanical properties of Al-Al₂O₃ micro and nano composites fabricated by stir casting. *Materials Science and Engineering: A*, 528(29–30), 8765–8771. <https://doi.org/10.1016/j.msea.2011.08.052>
- Tjong, S. C. (2007). Novel Nanoparticle-Reinforced Metal Matrix Composites with Enhanced Mechanical Properties. *Advanced Engineering Materials*, 9(8), 639–652. <https://doi.org/10.1002/adem.200700106>
- Zaiemyekheh, Z., Liaghat, G. H., Ahmadi, H., Khan, M. K., & Razmkhah, O. (2019). Effect of strain rate on deformation behavior of aluminum matrix composites with Al₂O₃ nanoparticles. *Materials Science and Engineering: A*, 753, 276–284. <https://doi.org/10.1016/j.msea.2019.03.052>